Astronomy
&
Astrophysics

Extragalactic globular clusters in the near infrared
III. NGC 5846 and NGC 7192[⋆,⋆⋆]

Quantifying the age distribution of sub-populations

M. Hempel[1], M. Hilker[2], M. Kissler-Patig[1], T. H. Puzia[3], D. Minniti[4], and P. Goudfrooij[5]

[1] European Southern Observatory, Karl-Schwarzschild-Str. 2, 85748 Garching, Germany
    e-mail: mkissler@eso.org
[2] Sternwarte der Universität Bonn, Auf dem Hügel 71, 53121 Bonn, Germany
    e-mail: mhilker@astro.uni-bonn.de
[3] Sternwarte der Ludwigs-Maximilians-Universität, Scheinerstr. 1, 81679 München, Germany
    e-mail: puzia@usm.uni-muenchen.de
[4] Departamento de Astronomía y Astrofísica, P. Universidad Católica, Casilla 306, Santiago 22, Chile
    e-mail: dante@astro.puc.cl
[5] Space Telescope Science Institute, Instrument Division, 3700 San Martin Drive, Baltimore MD 21218, USA
    e-mail: goudfroo@stsci.edu

Abstract. In this third paper of our series on near-IR and optical photometry of globular cluster systems in early-type galaxies we concentrate on the photometric results for NGC 5846 and NGC 7192, two group ellipticals, and on a first comparison between the globular cluster systems investigated so far. In NGC 5846 the colour-colour diagram shows clear bi-modality in $(V - K)$, which is confirmed by a KMM test. The mean colour of both peaks were estimated to be $(V - K)_{blue} = 2.57 \pm 0.06$ and $(V - K)_{red} = 3.18 \pm 0.06$. The situation in NGC 7192 is different, in that the colour-colour diagram gives no evidence for a distinct second population of globular clusters. Using simulated colour distributions of globular cluster systems, we make a first step in quantifying the cumulative age distribution in globular cluster systems. Also here the result for NGC 5846 leads us to the conclusion that its metal-rich globular cluster population contains two globular cluster populations which differ in age by several Gyr. The age structure for NGC 7192 shows instead strong similarity with a single-age population.

Key words. galaxies: star clusters – galaxies: individual: NGC 5846, NGC 7192

1. Introduction

As shown by many studies during the last decade (Zepf & Ashman 1993; Ashman & Zepf 1998; Kundu & Whitmore 2001a,b; Larsen et al. 2001; Kissler-Patig et al. 2002) globular cluster systems are a very powerful tool in galaxy formation and evolution studies. Although there is a wide agreement about the existence of sub-populations in cluster systems regarding their metallicity and their age, the discussion about the origin of those populations is still ongoing.

Starting with Peebles & Dicke (1968) who assumed globular clusters to be the first objects formed in the early universe, the number of possible formation scenarios increased drastically since then. One of the main issues is to explain the multi-modality found in colour-colour diagrams of globular cluster systems. In general it is agreed that different globular cluster populations are produced during strong star formation events, but the nature of these events remains under debate. Besides the merger scenario, favoured by Ashman & Zepf (1993) (see also Ashman & Zepf 1992; Whitmore et al. 1993; Whitmore & Schweizer 1995; Schweizer et al. 1996; Kissler-Patig 2000), there is a number of alternatives, i.e. the accretion scenario (Côté et al. 1998; Côté et al. 2002; Hilker et al. 1999) or the monolithic collapse (Forbes et al. 1997a; Kissler-Patig et al. 1998, and references therein). From the photometric point of view it has been shown that the multi-modality of the colour distribution is a common feature of globular cluster systems

[⋆] Based on observations at the Very Large Telescope of the European Southern Observatory, Chile (Program 63.N-0287).

[⋆⋆] Based on observations made with the NASA/ESA Hubble Space Telescope, obtained from the data archive at the Space Telescope Science Institute. STScI is operated by the association of Universities for Research in Astronomy, Inc. under the NASA contract NAS 5-26555.

(Gebhardt & Kissler-Patig 1999). In particular, the existence of a blue, old and metal-poor cluster population (Ashman & Bird 1993; Burgarella et al. 2001) is a general feature. Regarding the red sub-population the almost only consensus which has been reached so far, is about the large varieties between different cluster systems. This includes the possible existence of sub-populations within the red population which is interpreted as a sign of different star formation events in later stages of the galaxy evolution.

The main problem in specifying and dating different star formation events arises from the age-metallicity degeneracy of the most commonly used optical colours. So far the bulk of high-quality photometric investigations have been performed using *Hubble Space Telescope (HST)* in the optical wavelength regime (Forbes et al. 1998; Kundu & Whitmore 1998; Gebhardt & Kissler-Patig 1999; Larsen et al. 2001). It has been shown (Minniti et al. 1996; Kissler-Patig 2000; Kissler-Patig et al. 2002 (hereafter cited as Paper I); Puzia et al. 2002 (hereafter Paper II)) that combining optical and near-infrared data is a more promising method to separate age and metallicity effects and to access the relative ages of the globular cluster populations. The method relies on a sampling effect, where the V-band is dominated by stars near the turn-off (TO) region, whereas the main contribution to the K-band is from giant branch stars (Yi et al. 2001). Whereas the TO is dominated by age effects, the giant branch shows a high sensitivity to metallicity (Saviane et al. 2000). This results in a similar dependence of $(V - I)$ and $(V - K)$ on the age of the clusters, but a higher sensitivity of $(V - K)$ to the metallicity.

In the previous two papers of this series (Papers I and II), a systematic survey of globular cluster systems of E and S0 galaxies in the combined optical and near-infrared wavelength range (using the V, I, and K_s bands) has been started. In Paper I, we compared the globular cluster systems of two ellipticals in the Virgo cluster, namely the giant central galaxy M 87 and an intermediate-luminosity galaxy NGC 4478. We found that in those cases, the $(V - K)$ colour distribution yielded roughly consistent conclusions relative to those derived from the $(V - I)$ colours measured by *HST*. In Paper II however, the $(V - K)$ colours of globular clusters in NGC 4365 led us to postulate the existence of a significant population of intermediate-age (~2–6 Gyr old), metal-rich globular clusters, which was not revealed by the $(V - I)$ colours. This important result has recently been confirmed by deep spectroscopy (Larsen et al. 2003), adding credibility to the results derived from our optical + near-infrared imaging program.

One of the aims of this series is to study the the globular cluster systems of galaxies in different environments, e.g. giant ellipticals in centres of clusters as well as rather isolated and less luminous galaxies. The present work will focus on NGC 5846, a giant E0 galaxy in the centre of the Virgo-Libra Cloud, and on NGC 7192, an isolated elliptical with only one companion. Basic informations on both galaxies are provided in Table 1.

Both systems have already been studied in the optical (Forbes et al. 1997b; Gebhardt & Kissler-Patig 1999), and show a very broad $(V - I)$ colour distribution. This work aims at the detection of different globular cluster sub-populations,

Table 1. General information about the host galaxies NGC 5846 and NGC 7192. The references are (1): de Vaucouleurs et al. 1991, (2): Schlegel et al. 1998, (3): Buta & Williams 1995, (4): Frogel et al. 1978, (5): Tonry et al. 2001.

Property	NGC 5846	NGC 7192	Reference
RA (J2000)	15h06m29s	22h06m50s	(1)
Dec (J2000)	+01°36′25″	−64°18′57″	(1)
$B_{T,0}$	10.87	12.19	(1)
E_{B-V}	0.055	0.034	(2)
$(B - V)_o$	0.96	0.92	(1)
$(V - I)_{eff,o}$	1.28 ± 0.01	1.24 ± 0.01	(3)
$(V - K)_{eff,o}$	3.51 ± 0.01		(4)
$(m - M)_V$	31.98 ± 0.20	32.89 ± 0.32	(5)
M_V	−22.07 ± 0.20	−21.62 ± 0.35	(1), (5)

the determination of their age structure and a first comparison of various globular cluster systems. The present paper is organised as follows. In Sect. 2 the observations and the data reduction procedures are described. Section 3 contains the main results of the observations and Sect. 4 describes our approach towards quantifying the age structure in globular cluster systems and the results for both systems. In Sect. 5 we will give an outlook on the upcoming work.

2. Observations and data reduction

2.1. VLT/ISAAC near–infrared data

The K_s band exposures for both galaxies have been taken in service mode (ESO program 63.N–0287) with the Near-Infrared Spectrometer And Array Camera (ISAAC) attached to the Unit Telescope 1 (Antu) of the European Southern Observatory's Very Large Telescope (VLT). The field-of-view of ISAAC's Rockwell infrared array is $2.5' \times 2.5'$, with a pixel scale of 0.147″/pixel. All data were obtained in April and June 1999 in different nights under varying photometric and seeing conditions. Standard star observations revealed that the conditions were not photometric during all nights and an adjustment (described below) was necessary to align all nights onto a photometric system. As in Papers I and II we will always refer to the K_s filter as K.

The NGC 5846 data were obtained during the nights of April 6th, 8th, and 9th 1999 while the NGC 7192 data were taken during the nights of June 1st, 2nd, 21st, and 22nd. The observing strategy for NGC 5846 data was the following: 10×10 s object + $5 \times (2 \times 10$ s) sky + 10×10 s object. The one for NGC 7192: 10×10 s object + $2 \times (6 \times 10$ s) sky + 10×10 s object. The monitoring of the seeing, magnitude variations, sky level and geometric correction was done by measuring the parameters of four isolated stars in each single frame for both galaxies. A detailed description of the sky subtraction and combination procedure of the K band data is given in Puzia et al. (2002). The *FWHM* of the stellar PSF in the final K-band image is ~0.4″ for NGC 5846 and ~0.5″ for NGC 7192. The total exposure times for NGC 5846 and NGC 7192 are 10 000 s, and 12 000 s, respectively.
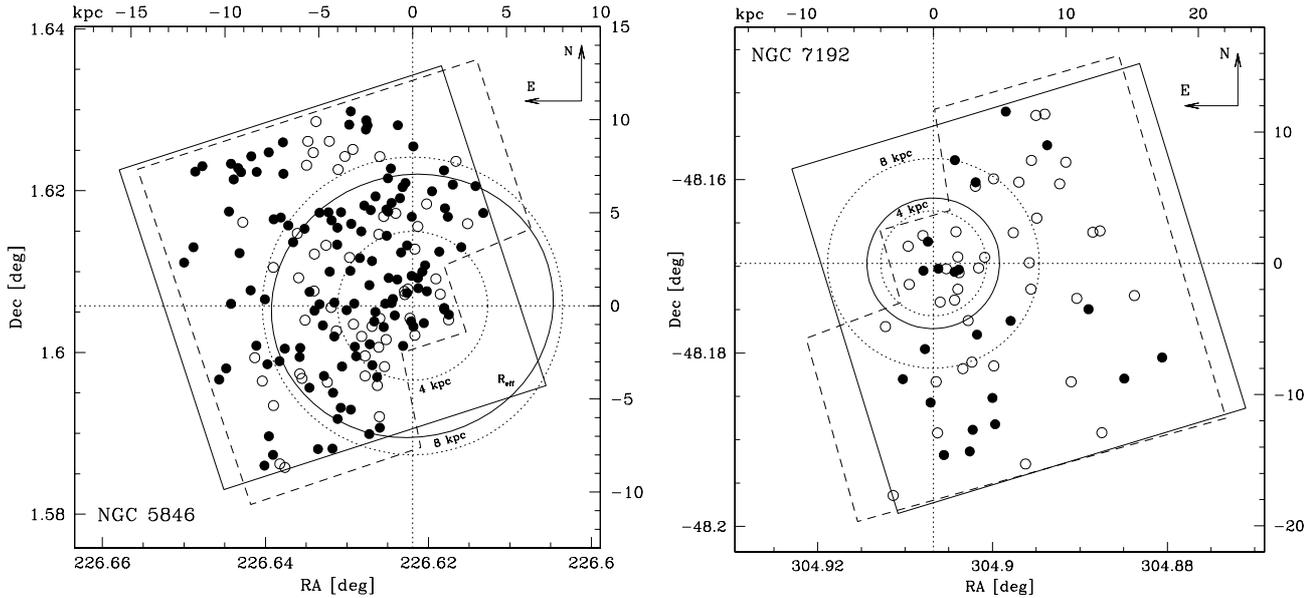
Fig. 1. Field of view of NGC 5846 (left) and NGC 7192 (right). The ISAAC field was chosen to fit the available archive data taken with WFPC2 onboard the HST. The dashed lines in both frames indicate the HST field and the solid one the corresponding ISAAC image. Dotted circles show the 4 and 8 kpc distance to the galactic centers, the solid circles the half light radii of the galaxy's light. The globular cluster samples were divided in two colour sub-populations. Dots mark objects with $0.8 \leq (V - I) \leq 1.2$ and open circles represent clusters in the range $1.2 < (V - I) \leq 1.5$.

2.1.1. Photometry

The photometric calibration of the NGC 5846 and NGC 7192 data set was based on the photometry of 3 and 4 near-IR standard stars, respectively (Persson et al. 1998).

Measuring the instrumental magnitudes in an aperture of 6 pixel diameter and applying the same analysis as described in Puzia et al. (2002), the following calibration relations for the photometric nights have been derived

$$K_{5846} = k_{\text{inst}} + 23.81(\pm0.018) - 0.05(\pm0.009)\chi \quad (1)$$

$$K_{7192} = k_{\text{inst}} + 23.83(\pm0.010) - 0.05(\pm0.007)\chi \quad (2)$$

where K_{galaxy} is the calibrated magnitude, k_{inst} is the instrumental magnitude, and χ the effective airmass (=1.23 for NGC 5846 and 1.34 for NGC 7192). The error of the zero points (second term in Eqs. (1) and (2)) includes photometric errors of each single standard star measurement and the errors of the aperture correction analysis. The error of the airmass term is an estimate from the variations in airmass of all single exposures.

The zero point shifts of the non-photometric nights to photometric conditions has been derived by tracing the magnitudes of four isolated stars over all nights. The final photometry was performed on the overall combined image. For NGC 7192 it was first done on two combined images separately. One for the photometric nights (June 1st and 2nd), and one for the non-photometric nights (June 21st and 22nd). The magnitudes of both images have been averaged after a zero point correction of the latter. The true photometric uncertainty, measured by the scatter of the single measurements is of the order of ≤0.04 mag, mainly due to the strongly varying sky background.

Finally, all magnitudes were corrected for Galactic foreground reddening using the reddening values of Table 1 and

the extinction curves of Cardelli et al. (1989). The corrections for NGC 5846 and NGC 7192 are $A_K = 0.020$ mag and $A_K = 0.012$ mag.

2.2. HST/WFPC2 optical data

The HST data were taken from the public HST archive. NGC 5846 was observed with HST + WFPC2 under program GO.5920. The total exposure times of the combined images are 6600 s in F555W, and 6900 s in F814W. NGC 7192 has been imaged with WFPC2 under program GO.5943 in F555W and F814W filters with 1300 s and 1000 s of total exposure time, respectively. The HST images were reduced and calibrated following the procedure as described in Puzia et al. (1999, 2002). All magnitudes were measured with the SExtractor tool using a 8 and 4-pixel-diameter aperture for the PC and WF chip and corrected with respect to the Holtzman 0.5″ standard aperture (Holtzman et al. 1995). Instrumental magnitudes were then transformed to the Johnson V and I magnitudes according to the prescription given by Holtzman et al. (1995). All magnitudes were reddening corrected using the following values: $A_V = 0.182$ and $A_I = 0.107$ for NGC 5846 and $A_V = 0.113$ and $A_I = 0.066$ for NGC 7192 (see E_{B-V} in Table 1).

2.3. Selection criteria

After combining the optical and near-infrared data using the GEOMAP task within IRAF, the globular cluster sample includes 184 and 61 objects for NGC 5846 and NGC 7192, respectively. Figure 1 shows the field of view for both galaxies

and the spatial distribution of the cluster candidates. In order to limit the contamination of the sample by background galaxies or foreground stars and to set a limit onto the photometric error, general selection criteria have been applied. In our discussion only objects with a photometric error $\Delta(V - I) \leq 0.1$ mag and $\Delta(V - K) \leq 0.1$ mag and a *FWHM* of the PSF below $0.25''$ in the V and I-band are considered.

3. Colour-colour diagrams for NGC 5846 and NGC 7192

Colour-colour diagrams together with various SSP models (e.g. in this paper by Bruzual & Charlot 2000) are the basis for age and metallicity estimates. Different models, at identical colors, can show differences in *absolute* age of about 3 Gyr. Thus, the SSP approach can only lead to approximate *absolute* ages for the sub-populations. However, *relative* ages can be estimated accurately enough to separate sub-populations built up during major star formation events.

As shown in Puzia et al. (2002), the various models differ mainly in the metal-rich range (approx. [Fe/H] > -0.8). A detailed comparison between the different models in an absolute sense can be found in Maraston et al. (2001). The metal-rich regime, however, is exactly the one we intend to probe, given that the intermediate-age populations are expected to be enriched in metals.

As opposed to the situation for absolute ages, the *relative* age predictions for given colors are relatively similar from model to model. Since we focus on the *relative* age dating of globular cluster systems the choice of a specific model is not crucial and we use the model of Bruzual & Charlot (2000) throughout the following analysis.

As we will show in the following two subsections the results of the KMM test (McLachlan & Basford 1988, updated version 2001) and the derived metallicities are found to differ significantly from expected values and even seem to be in contradiction to what visual inspection of the colour-colour diagrams tells us. Considering the relatively small sample size, the photometric errors in $(V - K)$ and the limited depth of the observations (shifting the peak position toward red colors) the results of the KMM test, as described by McLachlan & Basford (1988), have to be discussed with much caution. Since this work concentrates on relative ages at this stage we will only mention the results of the KMM and leave the discussion for later.

3.1. NGC 5846

The colour-magnitude diagram (hereafter CMD) and the colour-colour diagrams for NGC 5846 are given in Figs. 2 and 3. The histogram in the upper part of the CMD shows the complete set of clusters as a solid histogram whereas the selected objects, following the selection criteria given in Sect. 2.3, are shown by the hatched histogram. As expected the selection criteria affect mostly the objects in the very red colour range, since the photometric errors are larger and background galaxies possibly contaminate the sample.

The CMD (Fig. 2) reveals evidence for a bimodal colour distribution. The KMM test as described by Ashman et al. (1994) confirms this result with a confidence level of ~90% for a bimodal colour distribution. We obtain peak positions of $(V - K)_{blue} = 2.57 \pm 0.06$ and $(V - K)_{red} = 3.18 \pm 0.06$ for both colour populations with an estimate of correct allocation value (confidence level) of 0.79 and 0.94 for the blue and the red peak, respectively. Hereby about 30% of the globular clusters were assigned to the blue population and 70% to the red. Using the calibration by Kissler-Patig (Paper I) for old populations, this corresponds to a metallicity of [Fe/H] = -0.54 ± 0.6 dex and 0.27 ± 0.4 dex for the metal-poor and the metal-rich populations, respectively.

Note that our completeness limit is dominated by the K-band, and that we are biased in favour of red clusters (Paper II; see Fig. 2). Thus, both the ratio of the numbers of red to blue clusters and the metallicity of the blue peak are overestimates.

It is interesting to mention that no multi-modality could be found in the $V - I$ colour distribution. This is similar to the situation in NGC 4365 where the intermediate-age population, when projected on the $V - I$ axis, fills the gap between the two old (metal-rich and metal-poor) sub-populations. When forced to bimodality, the $(V - I)$ peak positions determined by the KMM test are $(V - I)_{blue} = 1.11$ and $(V - I)_{red} = 1.13 \pm 0.02$. This is in agreement with the results by Gebhardt & Kissler-Patig (1999).

3.2. NGC 7192

Referring to the CMD and the colour-colour diagram for NGC 7192 given in Figs. 4 and 5, the difference to the globular cluster system of NGC 5846 can be seen: while NGC 5846 exhibits a strong spread perpendicular to the isochrones, NGC 7192 is more homogeneously populated along the isochrone.

The small number of objects do not allow one to draw strong conclusions from the KMM test in terms of the existence of colour bimodality. The colour-colour plot for NGC 7192 does suggest the existence of two populations of different metallicity (i.e., a "metal-poor" population with $(V - I) < 1.1$ and $(V - K) < 2.8$ and a "metal-rich" population with $(V - I) > 1.0$ and $(V - K) > 2.8$) but the small number statistics do not allow one to support this firmly statistically.

Formally, the colour for the two peaks of the distribution projected on the $V - K$ axis is returned by KMM to be $(V - K) = 2.83$ and 2.89 (with 90% of the objects assigned to the first peak), if a bimodal distribution is assumed. Since the difference in colour between the two peaks is well below the photometric error it seems far-fetched to assume the existence of two distinct globular cluster sub-populations.

Therefore we assume that the NGC 7192 globular cluster system consists only of one dominant population. Following the calibration values by Kissler-Patig (Paper I) we derive a peak metallicity of [Fe/H] = -0.57 ± 0.37.
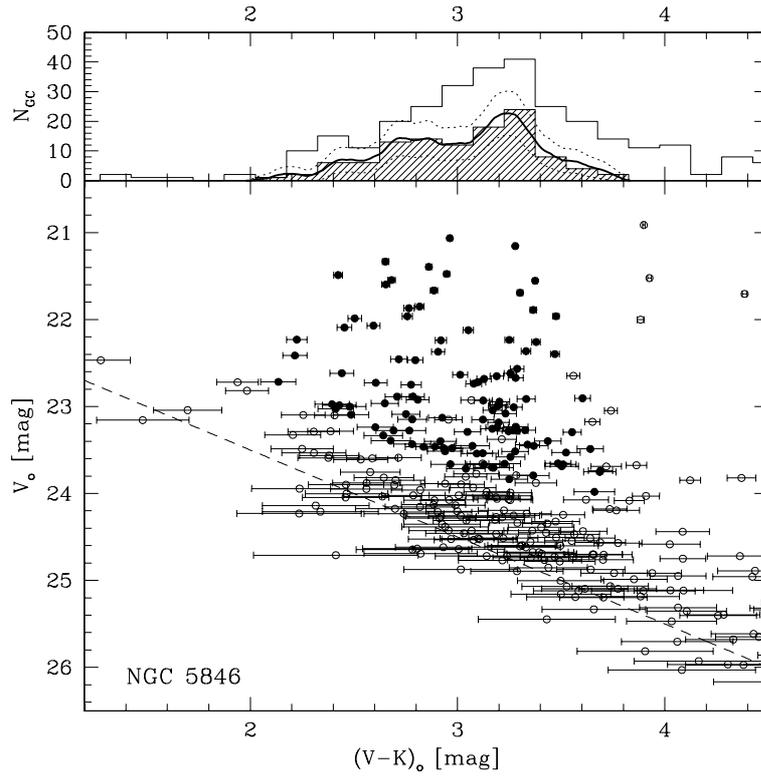
Fig. 2. V vs. $(V - K)$ colour-magnitude diagram for NGC 5846. The top sub-panel shows the colour distribution of all (open histogram) and selected (hashed histogram) objects. The solid line marks the probability density distribution together with its 1σ uncertainty (dotted line). The lower sub-panel shows the CMD. Here the filled symbols mark the selected clusters while open circles indicate rejected objects (see Sect. 2.3). Since the photometric errors are dominated by the K-band, only the $(V - K)$ errors are shown. The dashed line marks the limiting magnitude in the K-band ($K = 21.5$ mag).
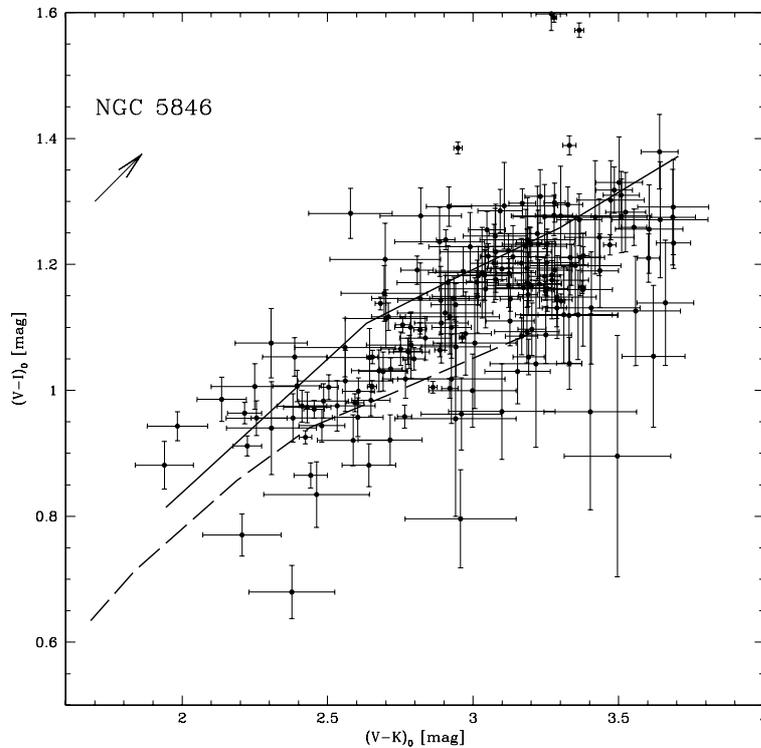
Fig. 3. $(V - I)$ vs. $(V - K)$ colour-colour diagram for NGC 5846. All data are corrected for Galactic foreground reddening. The reddening vector is marked by the arrow. As example the 15 Gyr and 2 Gyr isochrones (Bruzual & Charlot 2000) are marked by a solid and dashed line, respectively. As for NGC 4365 (Puzia et al. 2002) we find a second population of objects which are red in $(V - K)$ but intermediate in $(V - I)$ with $(V - I) \in [1.0, 1.2]$, and thus are clearly not compatible with old SSPs.
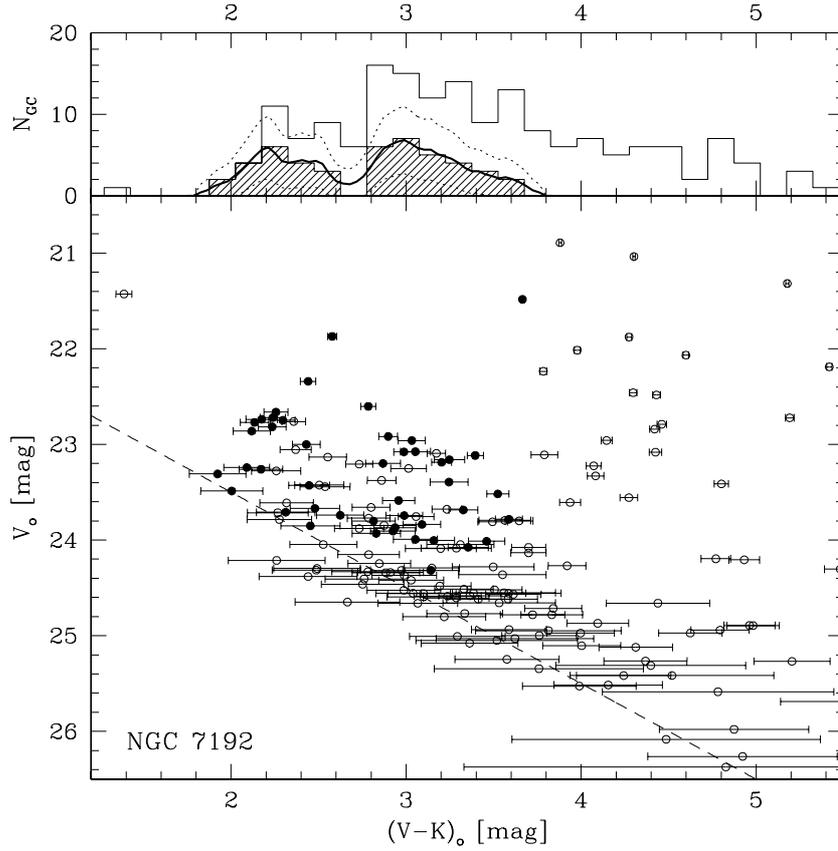
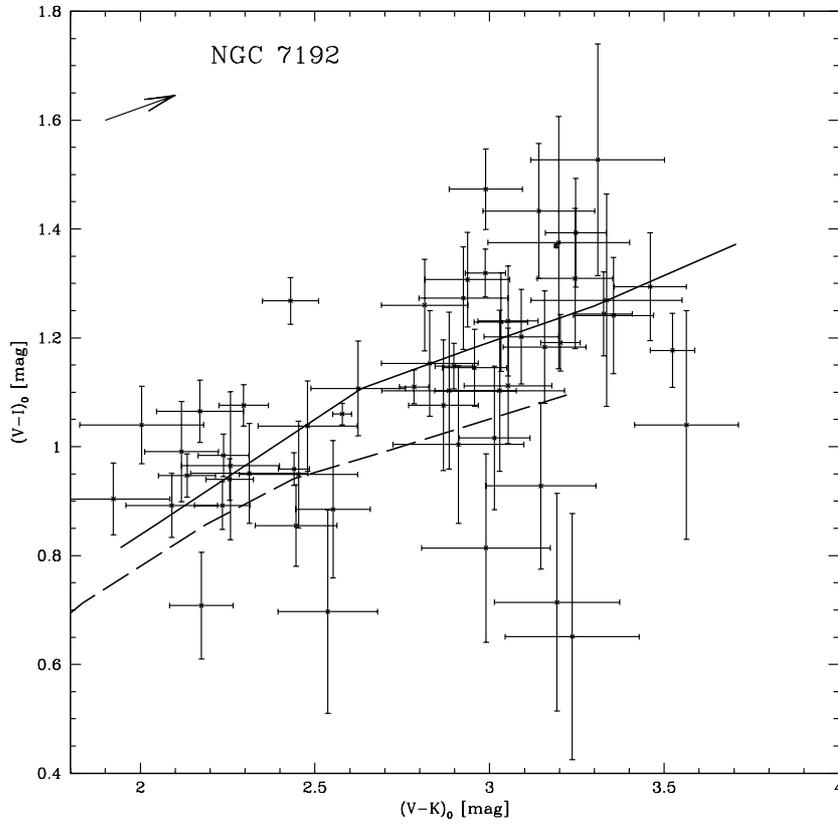**Fig. 4.** V vs. $(V - K)$ colour magnitude diagram for NGC 7192 (panels and symbols as in Fig. 2).

Fig. 5. Colour-colour diagram for NGC 7192. No clear indication for a second red sub-population can be found (isochrones as in Fig. 3).

Table 2. Fit parameter for model isochrones (Bruzual 2000) for a logarithmic fit $(V - I) = A \log(V - K) + B$.

Isochrone (Gyr)	1	2	3	5	7	10	13	15
A	0.5645	0.7136	0.7674	0.7795	0.7922	0.8134	0.8423	0.8573
B	0.3296	0.2809	0.2633	0.2765	0.2826	0.2766	0.2596	0.2502
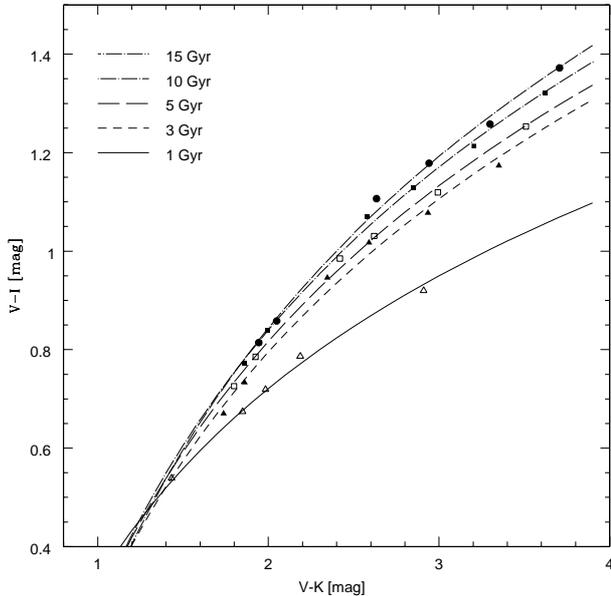
Fig. 6. SSP isochrone fit for $(V-I)$ vs. $(V-K)$ colour-colour diagrams. The symbols are colours given by the SSP models (Bruzual 2000) for 1 Gyr (open triangle), 3 Gyr (solid triangle), 5 Gyr (open square), 10 Gyr (solid square) and 15 Gyr (dots). The lines represent the result of a logarithmic fit to the isochrones with $(V - I) = A \log(V - K) + B$. The fit parameters A and B are given in Table 2.

4. Determining the age structure from colour-colour diagrams

4.1. Colour distributions

The basic idea in using optical and near-infrared photometry in globular cluster studies is to lift the age-metallicity degeneracy and to resolve possible age sub-populations of globular clusters. The minor drawback with respect to using optical colors alone is an increased photometric error mainly caused by the infrared observations, i.e., in the K-band. This, however, is more than compensated for by the larger diagnostic power of the optical – near-infrared combination (see Papers I and II). A separation in the colour-colour plot of sub-populations with different metallicities becomes easier, and a separation in age at a given metallicity becomes feasible.

We investigate below what the diagnostic power of the method is in terms of separating sub-populations of different ages. To do so, we investigated artificial colour-colour distributions of composite populations based on the Bruzual & Charlot (2000) isochrones. These artificial systems were built as follows:

• **In a first step** we create an artificial $V - K$ distribution of metal-rich globular clusters. We populate the red $(V-K)$ colour range $(2.7 \le (V - K) \le 3.8)$, assuming that it is occupied by "old" and "intermediate" age objects. We do not consider bluer clusters $(2.0 \le (V - K) \le 2.7)$, assuming that these are only "old" objects.

For now, we assume cases similar to NGC 5846 (see Fig. 3) in terms of sample size and photometric errors. For a first exemplary case, we assume 50% of the red population to be 15 Gyr old and 50% to be 3 Gyr old. These numbers are not assumed to reflect the "true" situation, but rather serve to demonstrate the method at this point. We will probe models with different ratios in the future (see Sect. 5.2). Further, it will become clear below that we are not directly comparing observed and simulated colour-colour diagrams but rather their cumulative age distributions, i.e., properties of the distributions still need to be "calibrated".

The final modeled systems contain 43 old, blue objects (not considered further) and 120 red objects homogeneously distributed within the $V - K$ range[1]. The red population was divided into an old (15 Gyr) and young (3 Gyr) population with 60 objects each.

• **In a second step** we attach to each $V - K$ data point a (1σ) error drawn randomly from our observed list of $\Delta(V - K)$ errors for NGC 5846, and then smear in a Monte-Carlo approach each $V - K$ point with up to ± 3 times its associated error (i.e. allowing up to 3σ errors in very rare cases). These new $V - K$ values are stored with their 1σ error and used for the further process.

• **The third step** consists of associating a $V - I$ colour to each new $V - K$ colour. To do this, we perform a least-square fit to the SSP model isochrones (in this case from Bruzual & Charlot 2000) by a logarithmic function $((V - I) = A \log(V - K) + B)$. The particular fit parameters A and B are given in Table 2. Figure 6 shows the isochrones as given by Bruzual (2000) and our fits to the isochrones (solid lines).

The fits are then used to compute for each $V - K$ point the corresponding $V-I$ point, once the age was chosen. In our case, we used the 15 Gyr fit for the 60 old artificial clusters, and the 3 Gyr fit for the other 60 (young) artificial clusters.

• *Finally, in* **the fourth step** we associate a measurement error $\Delta(V - I)$ to each $(V - I)$ data point in a similar way as for $(V-K)$. We now have a set of 120 objects (60 old, 60 young) with associated $(V - K)$ and $(V - I)$ colors and errors.

As an example of such artificial colour-colour distributions, we show in Fig. 7 the modeled colour-colour diagram of a purely 15 Gyr old population and a composite old (15 Gyr)

---

[1] We experimented also with Gaussian distributions within this colour range, but the final results of the experiment did not differ significantly and we have no better physical justification for a Gaussian than for a homogeneous colour distribution.
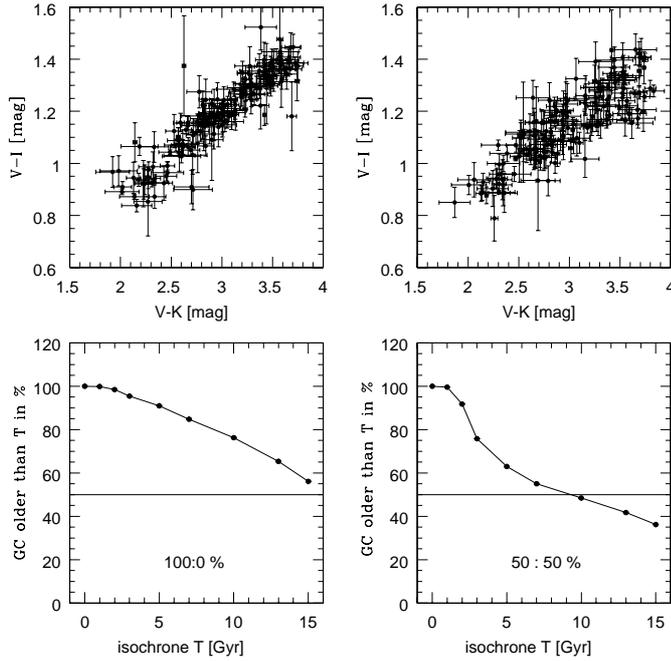
Fig. 7. The upper two panels show the $(V − I)$ vs. $(V − K)$ colour-colour diagram for a single age population (left panel) and a composite 50% old (15 Gyr) and 50% young (3 Gyr) cluster population (right panel). In the lower panels, the cumulative age structure (see Sect. 4.2) for both cases is given as the mean of 1000 such simulations. The 50%-level is marked as a solid line.
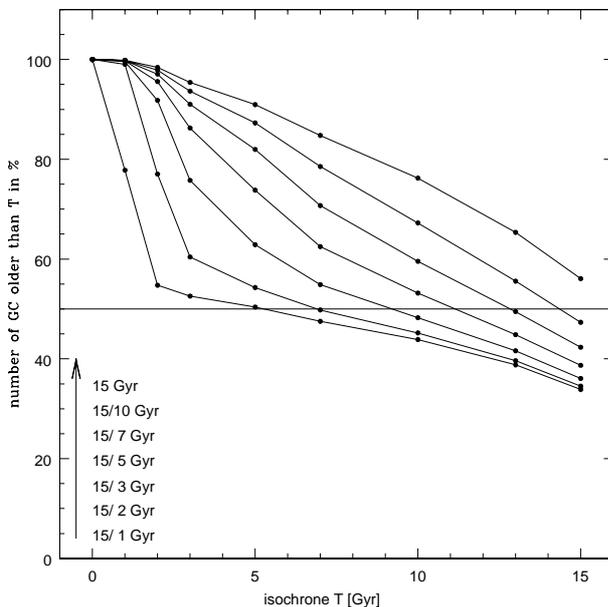

Fig. 8. Age distribution for mixed cluster populations assuming half of the objects being 15 Gyr old and half of them being respectively 1, 2, 3, 5, 7 or 10 Gyr old. The 50% level is marked by a solid line.

and young (3 Gyr) clusters as well as the resulting age distribution (lower panels). This distributions should be compared to the observed data for NGC 5846 in Fig. 3.

4.2. Cumulative age structure

The separation of the isochrones in Fig. 6 and the difference between the distributions in Fig. 7 (upper panels) motivated us to use the optical-near infrared photometry in order to try to separate globular cluster populations of different ages. This appears from the above plots to be at least possible to age differences of 10 Gyr or more (with respect to 15 Gyr for the oldest clusters). Therefore we decided to take the analysis one step further and to make a first attempt towards determining the age structure of the globular cluster systems.

We first attempted to compare directly the observed and the artificial colour-colour distributions, but this turned out to be too complicated. Two dimensional statistical tests are required in that case and the typical number of data points is not leading to any statistically significant results. We experimented with 2-dimensional f-test, 2-dimensional Kolmogorov-Smirnov tests, but in order to constrain the tests somewhat, one needs to put rather artificial constraints and the physical meaning of the final results is dubious.

We therefore decided to focus on 1-dimensional representations of the age structure. The dimension was chosen to maximize the age gradient along it, i.e., "perpendicular" to the isochrones.

Briefly, we associate to every cluster in our observed or artificial distribution an "age greater than X" when it lies above the isochrone of that age X in the colour-colour diagram. We start with the youngest isochrone (0 or 3 Gyr, see below) for which most cluster will lie above, and then move up isochrone by isochrone (in the steps 1, 2, 3, 5, 7, 10, 13, 15 Gyr). Hereby the notation "0 Gyr" refers to objects below the 1 Gyr isochrone. The result is an inverted cumulative distributions as shown in Fig. 8 for artificial distributions and in Fig. 9 for the observed distributions of all our galaxies analyzed so far. The cumulative age distribution can be represented in absolute numbers (left panel) or normalized to the total number of objects (at an arbitrary bin, right panel).

4.2.1. Artificial data sets

As described above, the first set of simulations was done for combinations of a 15 Gyr old sub-population and an equal number of intermediate-age objects (1, 2, 3, 5, 7, 10 Gyr). The results are shown in Fig. 8. Each curve shows the mean age structure as evaluated from 1000 models for that given age composition.

The realistic photometric errors create a spread in the colour-colour diagram such that even a pure 15 Gyr system does not show 100% of the clusters to be older than 15 Gyr. Instead, the spread in the $(V − I)$ vs. $(V − K)$ diagram leads to a gentle fall-off with isochrone age.

However, this fall-off clearly changes when a second, younger sub-population gets mixed in. By the time one mixes a 1, 2, 3 Gyr population in the system, the fall-off becomes very steep around 2, 3, 4 Gyr, and the curves cross the 50% level well before the 10 Gyr mark.
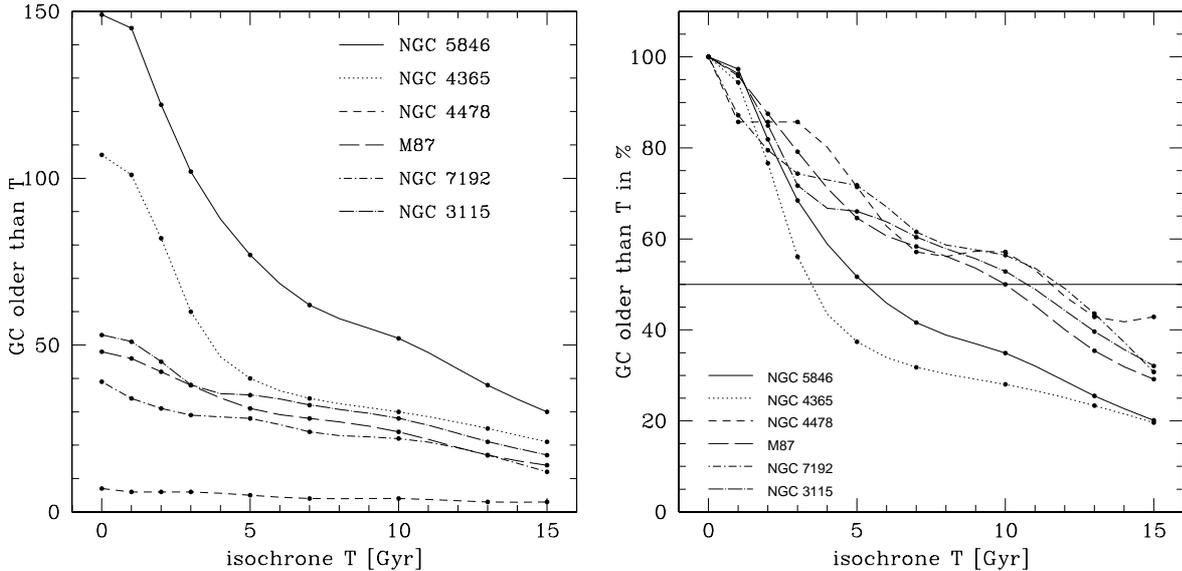
Fig. 9. Age distribution for different galaxies (see text). The absolute number counts (left panel) are normalised to the total numbers of clusters in the sample (right panel). It is clearly seen that two systems (NGC 5846, NGC 4365) are significantly different from NGC 4478, M 87, NGC 7192 and NGC 3115. This is interpreted as NGC 5846 and NGC 4365 hosting intermediate-age sub-population (which was confirmed spectroscopically for NGC 4365). The 50% level is marked by a solid line.

4.2.2. Observed data sets

The result for the artificial distributions can be compared with the observed age distributions of the globular cluster systems (see Fig. 9) in galaxies analyzed so far (M 87, NGC 4478, NGC 4365, NGC 3115, NGC 5846 and NGC 7192).

Taking first the observed data alone, we notice a clear similarity between NGC 5846 and NGC 4365, as opposed to the 4 other systems (see right panel of Fig. 9). Both galaxies fall-off steeply at early isochrone age and cross the 50% line well before 10 Gyr.

When compared to the results of artificial distributions, this leads immediately to the interpretation that both must host a significant fraction of intermediate-age clusters within their red sub-population. For NGC 4365, this was suspected already in Paper II and has since then been confirmed spectroscopically (Larsen et al. 2002).

In contrast, the age distribution of NGC 7192, NGC 3115, NGC 4478 and M 87 seems to be more consistent with what we would expect for a single age and old ($\geq$10 Gyr) population.

4.3. Contamination of background objects

Contamination of background objects is a potential problem in our analysis and we briefly investigate its impact below.

As above for the artificial distributions, we adopt a situation similar to the observations of NGC 5846. We used the Hubble Deep Field South (available at: www.stecf.org/hstprogrammes/ISAAC), which presents two advantages: it covers exactly the same (WFPC2) field of view as our observation, and it has a deep enough K-band observation to match our ISAAC observations of the globular cluster systems ($K < 21.5$ mag). The HDF-S sample was further selected in colours as for our samples. However, we could
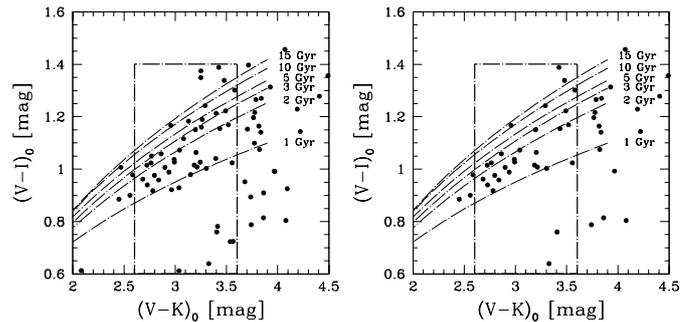

Fig. 10. ($V - I$) vs. ($V - K$) colour-colour diagram for the Hubble Deep Field-South using different K completeness limits: left, all objects with $K < 21.5$, right all objects with $K < 21.0$ (bracketing our completeness limit for NGC 5846). The box marks the colour range in ($V - I$) and ($V - K$) used for the determination of the globular cluster age structure as described in Sect. 4.2. Both diagrams show that the highest contamination of our sample is expected below the 2 Gyr isochrone. The isochrones superimposed are from Bruzual & Charlot SSP models (2000).

not apply a *FWHM* selection (having only the list of objects) so that the contamination is expected to be an overestimate. Even in that case, however, we show below that the effect is negligible for cases such as NGC 5846.

Figure 10 shows the colour-colour diagram of the HDF-S. Depending on magnitude selection, we have between 25 and 40 background objects in our colour selection box. The resulting cumulative age distribution for the HDF-S sample is shown in Fig. 11 and assigns about 50% of the objects to a population younger than 3 Gyr. Further, from the colour-colour plots, it becomes clear that the majority of these objects actually lie below the 2 Gyr line, being bluer in ($V - K$) and ($V - I$) than the intermediate-age, metal-rich globular clusters in NGC 5846. It is most probably dominated by a
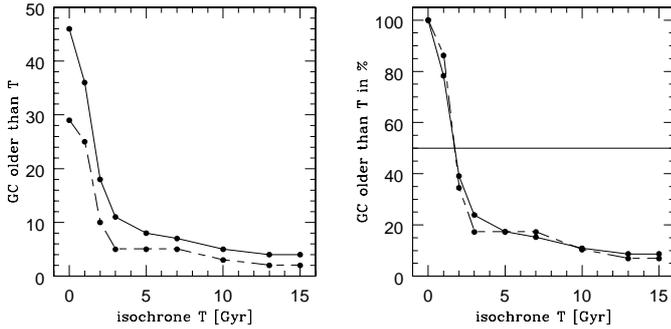
Fig. 11. Age structure of the HDF-South objects using the procedure given in Sect. 4.2. Left and right panels show the absolute and relative age distributions respectively. The colour selected samples with $K < 21.5$ and $K < 21.0$ are shown as solid and dashed curves, respectively. The 50% level is marked by a solid line.
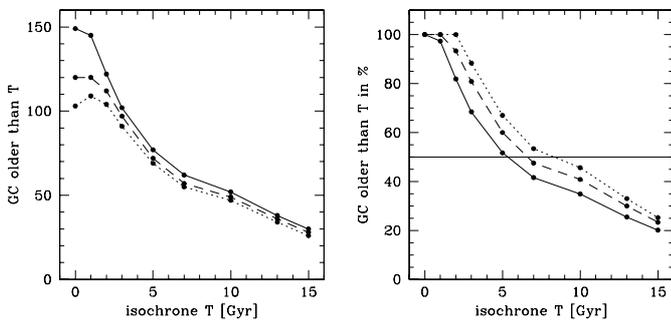

Fig. 12. Influence of background contamination on the age structure of the system in NGC 5846. The left and right panels show the absolute and relative cumulative age distributions, respectively. The uncorrected distribution is shown as a solid curve. The distribution corrected for background contamination of $K < 21.5$ and $K < 21.0$ are shown as long dashed and short dashed lines, respectively.

star-forming galaxy population that would be rejected by our *FWHM* criteria.

The effect of contamination on NGC 5846 is shown in Fig. 12. There, we plot the uncorrected (absolute and relative) age distributions, as well as the ones corrected for background contamination using the HDF-S source counts. Clearly, the effect is marginal. The contaminating objects tend to drag the age distribution towards younger ages, mimicking a slightly younger sub-population, e.g. the intersection with the 50%-level occurs at a larger age. Thus, "old" distribution such as for M 87, NGC 3115 etc would appear even older when corrected for contamination. In the cases of NGC 4365 and NGC 5846 (large numbers of clusters) the effect of this (over-estimated) contamination is small and does not influence the conclusion that these systems host a significant intermediate-age population.

5. Conclusions and future work

5.1. Conclusions

In this paper, we presented results of our optical – near-infrared study of the globular cluster systems of NGC 5846 and NGC 7192. While the latter does not show any significant anomaly, the former shows a case very similar to that of NGC 4365 (see Paper II) with good evidence for a significant

metal-rich, intermediate-age population in addition to an old, metal-rich one.

We developed a new method to quantify the age structure of the globular cluster systems studied so far, based on a comparison of the cumulative age distributions of the observed and modeled optical – near-infrared colour-colour diagrams. This method appears powerful enough to detect intermediate-age sub-population within globular cluster systems.

Our first conclusions for the galaxies studied so far are that both NGC 4365 and NGC 5846 have a cumulative age distribution of the metal-rich globular clusters that is different from those of the 4 other galaxies (NGC 3115, NGC 4478, NGC 7192 and M 87). The former are better modeled by a composite metal-rich population including an old (15 Gyr) as well as a significant young (1–5 Gyr) population. The others, in contrast, are very similar to the model for pure old populations and are thus best explained by being dominated by old objects.

NGC 7192 suffers from small number statistics, but the current dataset is, with respect to the colour-colour diagram and the age structure, more consistent with only one sub-population. Compared to the globular cluster systems investigated so far, NGC 7192 most closely resembles NGC 3115.

For M 87 and NGC 4478 the results given in Paper I were not fully conclusive. NGC 4478 also suffers from small number statistics. M 87 appears now more clearly dominated by two sub-populations differing in metallicity, but with a metal-rich population dominated by old objects (see also Jordán et al. 2002).

We need to emphasize again that the method cannot, currently, produce reliable *absolute* numbers, neither in terms of ages, nor in terms of ratios between the different populations. The results in this paper should therefore be considered as qualitative for now, and will be better quantified in the future.

5.2. Future work on age dating

The upcoming papers will analyze the remaining galaxies in our dataset (in total 11 galaxies). This will allow us to discuss the results in the light of galaxy properties. In particular, we will look at trends with galaxy size and environment. The local density (Tully 1988) covered by our galaxy sample spans from 0.08 Mpc^{-3} (NGC 3115) to 4.17 Mpc^{-3} (M 87) and environmental effects appear to be an important ingredient to galaxy formation and evolution.

On the modeling side, our goal is to improve the quantitative information of our method. We are developing a χ^2 test to find the best solution in the two parameter space of the models: ratio old/young and age of the young population, which are slightly degenerate. We also plan, with the help of spectroscopy and wide field photometry, to be able to better calibrate the models in terms of absolute age.

Also, we are exploring the dependence of the results on a particular SSP model and we will repeat the determination of the age structure using SSP models by Maraston (2000) and Vazdekis (1999). Further, we will investigate in more detail the

effect of background contamination. This latter aspects will be the subject of a separate paper.

References

Ashman, K. M., & Zepf, S. E. 1992, ApJ, 384, 50

Ashman, K. M., & Bird, C. M. 1993, AJ, 106, 2281

Ashman, K. M., Bird, C. M., & Zepf, S. E. 1994, AJ, 108, 2348

Ashman, K. M., & Zepf, S. E. 1998, Globular Cluster Systems (Cambridge: Cambridge University Press)

Ashman, K. M., & Zepf, S. E. 2001, AJ, 122, 1888

Bruzual, A. G., & Charlot, S. 1993, AJ, 405, 538

Bruzual, A. G. 2000, private communication

Burgarella, D., Kissler-Patig, M., & Buat, V. 2001, AJ, 121, 2647

Buta, R., & Williams, K. L. 1995, AJ, 109, 543

Cardelli, J. A., Clayton, G. C., & Mathis, J. S. 1989, ApJ, 345, 245

Côté, P., Marzke, R. O., & West, M. J. 1998, ApJ, 501, 554

Côté, P., West, M. J., & Marzke, R. O. 2002, ApJ, 567, 853

de Vaucouleurs, G., de Vaucouleurs, A., Corwin, H. G., et al. 1991, Third Ref. Catalogue of Bright Galaxies (New York: Springer)

Forbes, D. A., Brodie, J. P., & Grillmair, C. J. 1997, AJ, 113, 1652

Forbes, D. A., Brodie, J. P., & Huchra, J. 1997, AJ, 113, 887

Forbes, D. A., Grillmair, C. J., Williger, G. M., et al. 1998, MNRAS, 293, 325

Frogel, J. A., Persson, S. E., Matthews, K., et al. 1978, ApJ, 220, 75

Gebhardt, K., & Kissler-Patig, M. 1999, AJ, 118, 1526

Hilker, M., Infante, L., & Richtler, T. 1999, A&AS, 138, 55

Holtzman, J. A., Burrows, C. J., Casertano, S., et al. 1995, PASP, 107, 1065

Jordán, A., Côte, P., West, M. J., et al. 2002, ApJL, accepted [astro-ph/0207657]

Kissler-Patig, M., Forbes, D. A., & Minniti, D. 1998, MNRAS, 298, 1123

Kissler-Patig, M. 2000, Rev. Mod. Astron., ed. Schielicke, 13, 13

Kissler-Patig, M., Brodie, P. B., & Minniti, D. 2002, A&A, 391, 441 (Paper I)

Kundu, A., & Whitmore, B. C. 1998, AJ, 116, 2841

Kundu, A., & Whitmore, B. C. 2001, AJ, 121, 2950

Kundu, A., & Whitmore, B. C. 2001, AJ, 122, 1251

Larsen, S. S., Brodie, J. P., Huchra, J. P., et al. 2001, AJ, 121, 2974

Larsen, S., Brodie, J. P., Beasley, M. A., et al. 2003, ApJ, in press [astro-ph/0211434]

Maraston, C. 1998, MNRAS, 300, 872

Maraston, C. 2000, priv. communication

Maraston, C., Greggio, L., & Thomas, D. 2001, Ap&SS, 276, 893

McLachlan, G. J., & Basford, K. E. 1988, Mixture Models (Marcel Dekker Inc.)

Minniti, D., Alonso, M. V., Goudfrooij, et al. 1996, ApJ, 467, 221

Peebles, P. J. E., & Dicke, R. H. 1968, ApJ, 154, 891

Persson, S. E., Murphy, D. C., Krzeminski, W., et al. 1998, AJ, 116, 2475

Puzia, T. H., Kissler-Patig, M., Brodie, J. P., et al. 1999, AJ, 118, 2734

Puzia, T. H., Kissler-Patig, M., Brodie, J., et al. 2001, in Extragalactic Star Clusters, ed. D. Geisler, E. K. Grebel, & D. Minniti, IAU Symp., 207, 294

Puzia, T. H., Zepf, S. E., Kissler-Patig, et al. 2002, A&A, 391, 453 (Paper II)

Saviane, I., Rosenberg, A., Piotto, G., & Aparicio, A. 2000, A&A, 355, 966

Schlegel, D. A., Finkbeiner, D. P., & Davis, M. 1998, ApJ, 500, 525

Schweizer, F., Miller, B. W., Whitmore, B. C., et al. 1996, AJ, 112, 1839

Tonry, J. L., Dressler, A., Blakeslee, J. P., et al. 2001, ApJ, 546, 681

Tully, R. B. 1988, Nearby Galaxies Catalog (Cambridge: Cambridge University Press)

Vazdekis, A. 1999, ApJ, 513, 224

Whitmore, B. C., Schweizer, F., Leitherer, C., et al. 1993, 106, 1354

Whitmore, B. C., & Schweizer, F. 1995, AJ, 109, 960

Yi, S., Demarque, P., Kim, Y., et al. 2001, ApJS, 136, 417

Zepf, S. E., & Ashman, K. M. 1993, MNRAS, 264, 611